Taylor & Francis
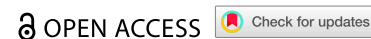Taylor & Francis Group

RESEARCH PAPER

🔓 OPEN ACCESS | Check for updates

CDP-DAG synthases regulate plant growth and broad-spectrum disease resistance

Ronglei Tan [a#], Gan Sha [a,b#], Qiuwen Gong[a], Lei Yang[a], Wei Yang[a], Xiaofan Liu[c,d], Yufei Li[e], Jiasen Cheng[c,d], Xin Qiao Du[f], Hongwei Xue[f,g], Qiang Li[h], Jie Luo[e,i], and Guotian Li [a]

[a]National Key Laboratory of Agricultural Microbiology, Hubei Hongshan Laboratory, Hubei Key Laboratory of Plant Pathology, The Center of Crop Nanobiotechnology, Huazhong Agricultural University, Wuhan, China; [b]National Key Laboratory of Green Pesticide, Guangdong Province Key Laboratory of Microbial Signals and Disease Control, South China Agricultural University, Guangzhou, China; [c]State Key Laboratory of Agricultural Microbiology, Hubei Hongshan Laboratory, Wuhan, China; [d]Hubei Key Lab of Plant Pathology, College of Plant Science and Technology, Huazhong Agricultural University, Wuhan, China; [e]School of Breeding and Multiplication (Sanya Institute of Breeding and Multiplication), Hainan University, Sanya, China; [f]Shanghai Collaborative Innovation Center of Agri-Seeds, Joint Center for Single Cell Biology, School of Agriculture and Biology, Shanghai Jiao Tong University, Shanghai, China; [g]College of Agricultural, South China Agricultural University, Guangzhou, China; [h]National Key Laboratory of Crop Genetic Improvement, Huazhong Agricultural University, Wuhan, China; [i]Yazhouwan National Laboratory, Sanya, China

ABSTRACT

Phosphatidic acid (PA) functions as a cell membrane component and signaling molecule in plants. PA metabolism has multiple routes, in one of which PA is converted into cytidine diphosphate diacylglycerol (CDP-DAG) by CDP-DAG synthases (CDSs). *CDS* genes are highly conserved in plants. Here, we found that knock-down of the *CDS* gene enhanced the resistance of *Arabidopsis thaliana* to multiple pathogens, with a growth penalty. When *Arabidopsis* leaves were treated with chitin or flg22, reactive oxygen species (ROS) production in *cds* mutants was significantly higher than that in the wild-type (WT). Similarly, phosphorylation of mitogen-activated protein kinases (MAPKs) in the *cds1cds2* double mutant was significantly increased compared to the WT. By integrating lipidomics, transcriptomics, and metabolomics data, PA accumulation was observed in mutants *cds1cds2*, activating the jasmonic acid (JA) and salicylic acid (SA) signaling pathway, and increasing transcript levels of plant defense-related genes. Significant accumulation of the downstream metabolites including serotonin and 5-methoxyindole was also found, which plays important roles in plant immunity. In conclusion, our study indicated the role of CDSs in broad-spectrum disease resistance in *Arabidopsis* and that CDSs are involved in plant metabolic regulation.

1. Introduction

Phospholipids, as amphipathic molecules, are major structural components of biological membranes and play vital roles in membrane trafficking. Some phospholipids such as phosphatidic acid (PA), function in signal transduction.[1] Phospholipids are involved in plant growth, development, and responses to biotic stress, by binding downstream proteins through lipid-protein interactions and modulating their expression levels, subcellular localization, or protein functions.[2]

PA, the simplest yet key phospholipid molecule, is highly dynamic and relays multiple cellular signaling events, including responses to biotic stress.[3] In plants, PA interacts with proteins that function in or outside cell nucleus to regulate cellular and physiological processes and plays indispensable roles in plant immunity.[1] PA binds to respiratory burst oxidase homolog D (RBOHD), which generates reactive oxygen species (ROS) in plant immunity, including both the pattern-triggered immunity (PTI) and effector-triggered immunity (ETI) processes. The binding of PA to RBOHD stabilizes RBOHD, thereby modulating ROS production.[4,5] As a dynamic molecule, PA is synthesized through multiple biochemical pathways, including the *de novo*-Kennedy pathway, and pathways involved in diacylglycerol kinases (DGKs) and phospholipase D (PLD).[6] In one of these ways, diacylglycerol kinase 5 (DGK5) catalyzes the synthesis of PA from diacylglycerol, and recent studies show that pathogen infection activates DGK5 to synthesize PA, which inhibits RBOHD protein degradation, thereby promoting ROS production and enhancing plant immunity.[4,7] In addition, PA binds to and inhibits abscisic acid (ABA) biosynthesis enzyme ABA2 and suppresses ABA production in response to abiotic stress in *Arabidopsis*.[8] It is clear from these studies that PA plays an important role in stress responses in *Arabidopsis*.

PA is the central precursor for all glycerophospholipids and can be converted to cytidine diphosphate diacylglycerol (CDP-DAG), a vital metabolic intermediate, through the CDP-DAG synthases (CDSs), and then toward PI, phosphatidylglycerol (PG) and cardiolipin (CL) via different enzymatic reactions.[9] There are five *CDS* genes in *Arabidopsis*, complete loss of expression of two of them *CDS1* and *CDS2* cause seedling lethality. *CDS3* is specifically expressed in certain plant structures such as stamens and mature pollen,[10] whereas CDS4 and CDS5 are localized at the plasma membrane, where there are important for PG synthesis in chloroplast-like vesicle

---

structures.[11] To study *Arabidopsis CDS1* and *CDS2* in detail, a *cds1cds2* knock-down line was generated.[12] This line exhibits reduced auxin levels and aberrant polar distribution of PIN1, leading to delayed embryonic development. Furthermore, the *cds1cds2* mutant show enhanced resistance to the oomycete pathogen *Phytophthora capsici*.[13] The *CDS1* homologue from rice, *RBL1*, negatively regulates rice immunity. When *RBL1* is deleted or mutated in rice, a strong autoimmune response is observed, with an increased level of PA and decreased levels of PI and its derivatives. Rice *rbl1* mutants show enhanced resistance to the rice blast fungus *Magnaporthe oryzae* and the bacterial blight pathogen *Xanthomonas oryzae* pv. *oryzae*.[13] However, how CDSs regulate plant growth, development and immunity is largely unknown. Here, we investigated the role of *Arabidopsis* CDSs in plant growth and broad-spectrum disease resistance by integrating transcriptomics, lipidomics and metabolomics approaches.

2. Materials and methods

2.1. Plant materials, strains and growth conditions

The *Arabidopsis thaliana* ecotype Columbia (Col-0) was used as the background of all lines used in this study. The *cds1* (SALK_001496) and *cds2* (SALK_106246) were obtained from Nottingham Arabidopsis Stock Centre. The *cds1cds2* double mutant was obtained by crossing homozygous *cds1* and *cds2*. All seedlings were grown in potting soil mix (peat soil: rich soil: vermiculite of 1:1:1, v/v/v) in a humidity plant growth chamber at 22°C, 60% humidity, with a photoperiod of 16:8 hours (h) light: dark.[12] *Botrytis cinerea* B05.10 (*B. cinerea*) and *Sclerotinia sclerotiorum* 1980 (*S. sclerotiorum*) were obtained from Prof. Long Yang[14] and Prof. Jiasen Cheng,[15] respectively. The *S. sclerotiorum* strain was cultured on potato dextrose agar (PDA) plates at 25°C for 3–4 d in the dark. The *B. cinerea* strain was cultured on PDA plates at 20°C for 2–3 d in the dark. *Pseudomonas syringae* pv. *tomato* DC3000 (*Pst* DC3000) was obtained from Prof. Xiufang Xin.[16] *Pst* DC3000 strains were incubated with 5 mL liquid LB medium at 28°C overnight, reaching a cell density of $OD_{600} = 0.8\sim1.0$.

2.2. Plant infection assays

Infection assays of *Arabidopsis* with *S. sclerotiorum* and *B. cinerea* were conducted as previously described with minor modifications.[14,15] Four-week-old leaves of *Arabidopsis* were used for pathogen inoculation. Fully extended *Arabidopsis* leaves were detached, surface-sterilized with 75% ethanol and placed on 0.8% water agar plates. Subsequently, mycelial blocks (2 mm × 2 mm) of *S. sclerotiorum* and *B. cinerea* were inoculated in the center of each leaf. The infected leaves were then kept at 25°C in the dark. At 30 hours post-inoculation, the infected leaves were photographed and the lesion areas were measured. Infection assays with *Pst* DC3000 were conducted as previously described.[17] *Pst* DC3000 were incubated with 5 mL liquid LB medium at 28°C overnight, reaching a cell density of $OD_{600} = 0.8\sim1.0$. Bacteria cultures were then harvested through centrifugation (4000 rpm, 25°C for 5 min), washed with sterile water, and diluted to a cell density of $OD_{600} =$

0.0005. The bacteria suspensions were infiltrated into the leaves using a needleless syringe, and the plants were subsequently covered with a clear plastic cover to maintain high humidity levels for 6 h. For each biological replicate two leaf discs (6 mm in diameter) were obtained from different leaves and surface-sterilized with 75% ethanol. The leaf discs were mashed and suspended in sterile water, the bacterial suspensions of different dilution ratios were prepared and then plated on TSA agar plates supplemented with 50 mg/L rifampicin. Colonies were counted after 48 h of incubation at 28°C.

2.3. Measurement of ROS

ROS was measured as previously described.[18] For ROS burst assay, 3-week-old leaves of the *Arabidopsis* plants were excised into 3 mm × 3 mm discs. These leaf discs were submerged in double-distilled sterile water in a 96-well plate and incubated overnight under controlled light conditions to counteract the wounding effects. After the incubation was finished, distilled water was replaced with a solution containing 50 μM luminol, 10 μg/ml horseradish peroxidase, and indicated elicitors (either 120 nM chitin or 200 nM flg22) or distilled water (as the blank). Chemiluminescence was measured at 500-ms intervals continuously over a period of 40 min on a SPARK-10 M microplate reader (TECAN).

2.4. RNA extraction and RT – qPCR assays

Leaves from 3-week-old *Arabidopsis* plants for each genotype were excised and immediately snap-frozen in liquid nitrogen. Total plant RNA was isolated using TRIzol (Vazyme). The separation of the organic and aqueous phases is facilitated with chloroform. The total RNA was precipitated from the aqueous phase using Isopropanol. HiScript II Q RT SuperMix for qPCR (Vazyme) was used to remove residual genomic DNA and synthesize complementary DNA.[13] The RT-qPCR analysis was performed using SYBR Green mix with a Bio-Rad CFX96 Real-Time System coupled to a C1000 Thermal Cycler. All the primer information for RT – qPCR assays are provided in Supplementary Table 1. *Arabidopsis MPK3* (AT3G45640), *MPK4* (AT4G01370), and *MPK6* (AT2G43790) genes encode three mitogen-activated protein kinases (MAPK), play critical roles in plant disease resistance by regulating multiple defense responses. *Arabidopsis ACTIN2* (AT3G18780) gene was used as the internal control to normalize the expression level of *MPK3*, *MPK4*, and *MPK6* genes for gene expression analysis. Furthermore, the expression level of target genes was quantitatively assessed using the $2^{-\Delta\Delta CT}$ method.[19]

2.5. MAPK phosphorylation assays

Two-week-old *Arabidopsis* plant grown on 1/2 MS plates were used for MAPK phosphorylation analysis. We placed 4–6 seedlings into sterile water overnight before the treatment, then immersed the roots of the seedlings in a solution containing indicated elicitors (120 nM chitin or 200 nM flg22) and incubated for 15 min. Each sample was collected in a centrifuge tube with liquid nitrogen and thoroughly ground to fine powder. The samples were

solubilized in the extraction buffer (50 mm Tris-HCl, pH 7.5, 150 mm NaCl, 1 mm EDTA, 1% Triton X-100, 0.5 mm PMSF and 1% protease inhibitor cocktail) and boiled at 95°C for 10 min. The protein extracts were centrifuged at 12,000 rpm at 4°C for 5 min.[20] A 20-μl mixed sample (containing 14-μl protein extract, 2 μl 0.4 M DTT, 4 μl 5×SDS loading buffer) was loaded on a 10% SDS – PAGE gel. The fractioned proteins were transferred to the PVDF membrane for immunoblotting. Blots were blocked with 5% BSA prepared in TBST at room temperature for 1 h, and then incubated with anti-phospho-p44/42 antibody (Cell Signaling Technology, 1:2000 dilution) overnight at 4°C. Subsequently, the blots were probed with a secondary antibody Goat anti-rabbit IgG HRP (Cell Signaling Technology, 1:5000 dilution) at room temperature for 1 h. The phosphorylated MAPK (pMAPKs) proteins were then visualized using ECL Chemiluminescence Kit (Vazyme., catalog no. E423) on the ChemiDoc Touch Imaging System (Bio-Rad). *Arabidopsis* ribulose bisphosphate car-boxylase/oxygenase (RUBISCO) was used as the internal control.[16]

2.6. RNA-seq analysis

Leaf samples from 4-week-old *Arabidopsis* plants were used for RNA-seq analysis. The 2×150-bp paired-end sequencing was performed on the BGISEQ-500 sequencer (BGI, Shenzhen, China). Raw sequencing data was filtered by removing sequencing adapters, low-quality reads (base quality less than or equal to five) and reads with high percentage of unknown bases ('N' base > 5%), and the resultant clean data were stored in the FASTQ format for downstream analysis. Clean reads were aligned against the *Arabidopsis* Col-0 genome using HISAT2.[21] Quantification of gene expression was performed using FeatureCounts. DESeq2 (version: 1.32.0) was used to assess differential expression between sample groups. Differentially expressed genes (DEGs) were identified by applying a |Fold Change| $\geq$ 1 and false discovery rate (FDR) $\leq$ 0.05. DEGs were functionally annotated using the GO data-base (http://geneontology.org/).[22]

2.7. Lipid extraction and analysis

Leaf samples from 4-week-old *Arabidopsis* plants were used for phospholipid extraction. Briefly, around 10 mg of fresh *Arabidopsis* leaf tissues were incubated in preheated isopropa-nol (75 °C) containing 0.01% butylated hydroxytoluene (BHT) for 15 min. After cooling to room temperature, chloroform was added to the samples, and then incubated with shaking at room temperature for 1 h. Lipid extracts were transferred to new glass tubes to repeat the extraction procedure until the leaf sample became bleached. 1 M KCl and water immediately added, and the upper phase was discarded after centrifugation (4°C, 1,000 g for 10 min). The lipid extracts were combined and evaporated under nitrogen gas, and then redissolved in chloro-form to a final concentration at 10 mg/ml.[23,24] Phospholipids were measured with an electrospray ionization source in posi-tive-ion mode.[25]

2.8. Metabolite profiling analysis

Freeze-dried tissue samples were ground into fine powder in a ball mill, and 50 mg of powder for each sample was mixed with 5 mL methanol/water (3:1, v/v), and incubated at 4°C overnight for water-soluble metabolites. Then, all samples were centrifuged at 10,000 g at 4°C for 10 min. The extracts were absorbed (CNWBOND Carbon-GCBSPEC cartridge) and filtered before liquid chromatography tandem-mass spectro-metry (LC-MS/MS) analysis.[26] The extracted samples were assayed by a Quadrupole Time of Flight (QTOF) system (TripleTOF 5600+; AB Sciex, USA) for untargeted detection and a QTrap system (QTRAP 6500+; AB Sciex) for targeted detection as described previously before.[27]

## 2.9. Quantification of total salicylic acid (SA) in leaves

Leaf samples from 4-week-old *Arabidopsis* plants were used for total SA analysis. Leaf tissues were collected and subjected to freeze-drying to preserve their biochemical content. Approximately 20 mg of the freeze-dried leaf tissues were pul-verized using liquid nitrogen, then mixed with 1 ml of 80% methanol and sonicated at 70°C for 15 minutes to extract the SA. After centrifuging the mixture at 7,000 g for 4°C, the supernatant was collected and passed through a filter to remove any remaining particulates. The filtrate, along with serial dilutions of the SA standard, was analyzed using high-performance liquid chromatography (HPLC) coupled with tandem mass spectrometry (MS/MS). The concentration of SA in each sample was calculated by comparing the results to a calibration curve generated from the SA standard.[13]

3. Results

To investigate the function of *CDS1* and *CDS2* in growth regulation and immunity of *Arabidopsis*, the growth phenotype of *Arabidopsis* mutants with reduced transcription levels of *CDS1* and *CDS2* caused by T-DNA insertions[12] at mature stage was observed. At 40 days post-sowing, the height of the *cds1cds2* mutant (26.04 cm) was significantly lower than that of the WT (35.48 cm) (Figure 1a), with a 27% reduction (Figure 1b). The number of siliques in *cds1cds2* was signifi-cantly reduced by 51%, compared to that in the WT. The plant height and the number of siliques per plant in the *cds1* and *cds2* single mutant lines showed no difference relative to the WT (Figure 1b–d).

The infection assays of 4-week-old *cds* mutant lines aimed to further investigate the resistance levels of these mutants to multiple pathogens. In the assay, the mean lesion area caused by *S. sclerotium* in the *cds1cds2* mutant was 0.22 mm^2 (Figure 2a), which was 47% smaller than that of the WT (0.41 mm^2) (Figure 2a). In contrast, enhanced resistance to *S. sclerotium* has not been observed in single *cds* mutants, which mean lesion area were 0.41 mm^2 and 0.34 mm^2, respectively. The *cds1*, *cds2*, and *cds1cds2* mutant plants all exhibited enhanced resistance to *B. cinerea* (Figure 2b). The *cds1cds2* mutants, the *cds1* mutants, and the *cds2* mutants showed 32%, 27%, and 28% reductions, respectively, in lesion area compared to the WT (Figure 2b). *Pst* DC3000 infection

(a)

WT   *cds1*   *cds2*   *cds1cds2*

(b)

(d)

(c)
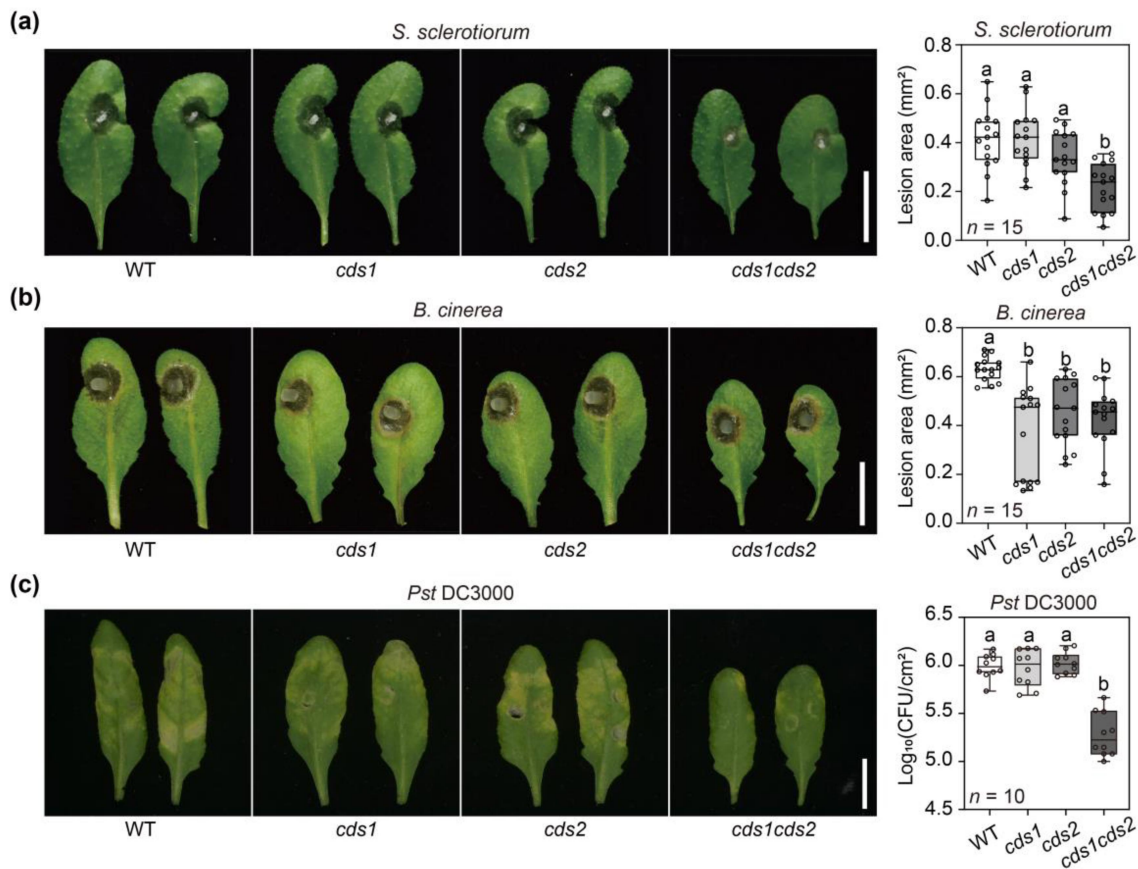

WT   *cds1*   *cds2*   *cds1cds2*
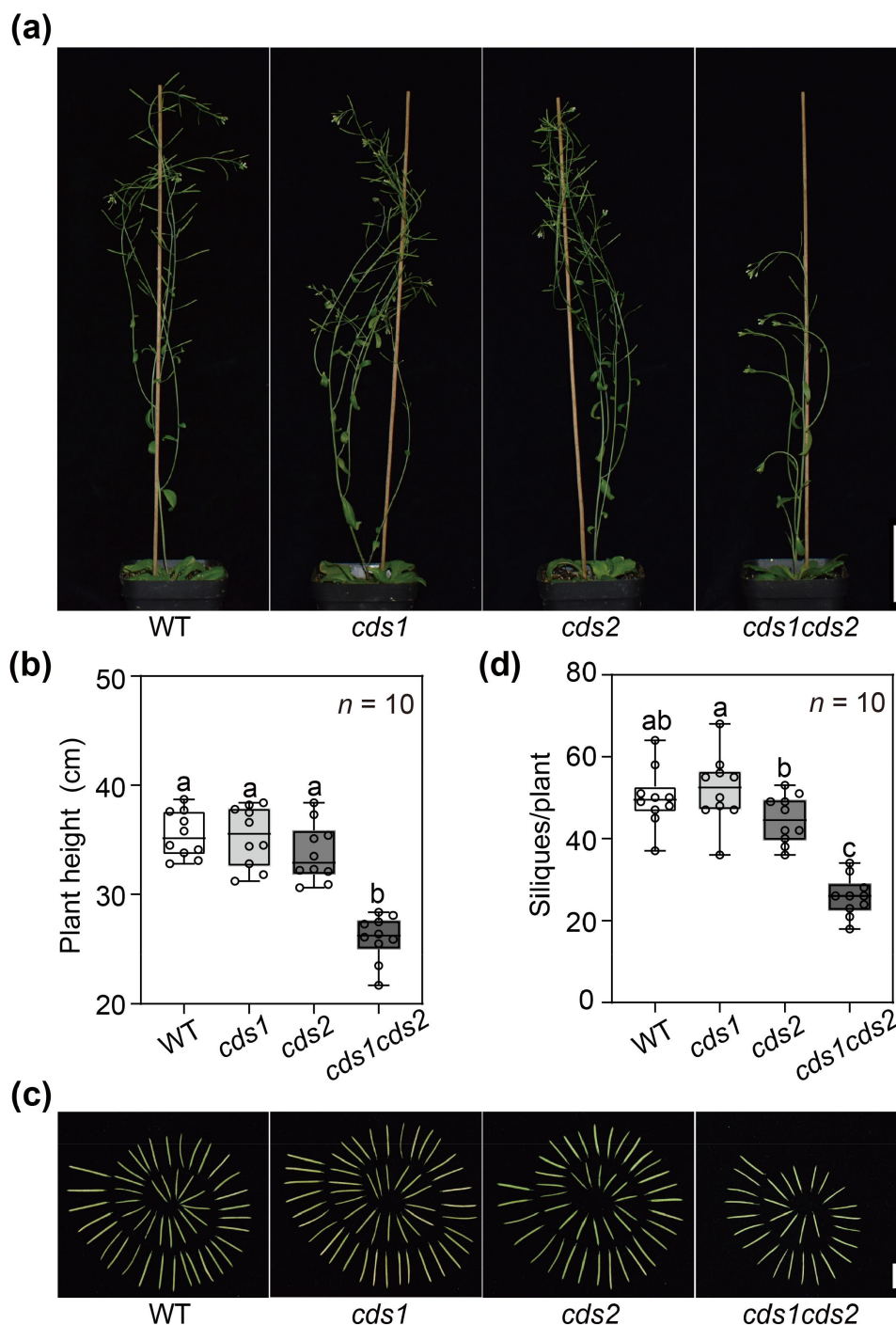
Figure 1. Plant growth is reduced in *Arabidopsis cds1cds2* mutants. (a) The *cds* mutant and wild-type (WT, col-0) plants at 40 days post-sowing (dps). Bar, 5 cm. Plants were grown in a growth chamber at 22°C, 60% humidity with a photoperiod of 16:8 hours (h) light: dark. (b) Plant height of *cds* mutants and WT. (c) Photograph of siliques from a representative plant and (d) The number of siliques per plant at 40 dps. Bar, 1 cm. Data are displayed as box and whisker plots with individual data points. The box plot elements are: center line, median; box limits, 25th and 75th percentiles. *n* indicates the number of biological replicates. Letters indicate statistically significant differences (ANOVA, $p \leq 0.05$). Duncan's multiple range test as method of *post-hoc* test.

assay showed that the *cds1cds2* mutants exhibited slightly smaller brown leaf spots compared to the WT and other lines (Figure 2c). Additionally, the colony-forming units (CFU) assay showed that the multiplication of *Pst* DC3000 was greatly restricted in *cds1cds2* mutants. The bacterial density within the leaves of WT, *cds1* mutant, and *cds2* mutant were 1.02×10^6 CFU/cm², 1.01×10^6 CFU/cm², and 1.08×10^6 CFU/cm², which were 5.6, 5.7, and 6 times compared to that of *cds1cds2* mutant (1.8×10^5 CFU/cm²),

respectively (Figure 2c). In summary, the *cds1cds2* mutant lines showed resistance to multiple pathogens.

A ROS bioassay of *cds* mutant lines, treated with pathogen-associated molecular patterns (PAMPs), was conducted to investigate the potential mechanisms underlying the enhanced disease resistance of the *cds1cds2* mutant. Under treatments of chitin and flg22, the ROS level in the *cds1cds2* mutant was 2.64- and 1.31- fold higher than that of the WT, respectively (Figure 3a). The total number of photons in the *cds1cds2*

Figure 2. *Arabidopsis cds1cds2* mutants show broad-spectrum pathogen resistance. (a) Infection assays with the *sclerotinia sclerotiorum* (*S. sclerotiorum*) and lesion areas of *cds* mutant lines at 30 hours post-inoculation (hpi); bar, 1 cm. (b) Infection assays with the *botrytis cinerea* (*B. cinerea*) and lesion areas at 30 hpi. (e) Bacterial infection assays with *Pseudomonas syringae* pv. *tomato* DC3000 (*pst* DC3000) at 3 days post-inoculation (dpi) and related bacterial populations. Box plot elements are: center line, median; box limits, 25th and 75th percentiles. *n* indicates the number of biological replicates. Letters indicate statistically significant differences (ANOVA, $p \leq 0.05$). Duncan's multiple range test as method of *post-hoc* test.

mutant showed 2.72- and 1.33- fold increase compared to that in the WT (Figure 3b). PTI often activates the downstream MAPK cascade immune response. The expression levels of *MPK3*, *MPK4*, and *MPK6* genes in *cds* mutant leaves were significantly upregulated compared to the WT (Figure 3c). Furthermore, total proteins from *cds* mutant leaf tissues treated with PAMPs were extracted to analyze the levels of pMAPKs using immunoblotting.[7] The accumulation levels of pMAPKs, the *cds1cds2* mutant showed significantly higher levels of pMAPKs than the WT (Figure 3d). SA, a key signaling molecule in plant immunity, induces disease resistance to various viruses, fungi and bacteria in plants. A significant increase in SA levels was detected in *cds1cds2* mutants, implying the important role of SA in enhancing disease resistance in *cds1cds2* mutants (Fig. S1). These results indicated that the *cds1cds2* mutant displayed a more robust immune response than the WT, and the enhanced disease resistance was associated with increased levels of ROS, pMAPKs and SA.

To investigate the underlying mechanisms by which *CDS* genes contribute to metabolism and defense, integrated transcriptomics, lipidomics, and metabolomics analyses of the *cds* mutant lines were conducted. To ensure the consistency of the results from the multi-omics association analysis, the leaves of *Arabidopsis* plants with the same growth condition were collected. Each analysis was performed with three biological replicates.[28] RNA-seq analysis showed that phospholipid biosynthesis and signaling genes, such as those involved in 'fatty acid response' and 'lipid response' were enriched in *cds1cds2* mutant lines. Signaling pathways associated with immunity, such as 'fungal response', 'JA response', and 'response to oxidative stress', were activated (Figure 4a). The upregulated expression of these genes likely enhanced the resistance of the *cds1cds2* mutant to different pathogens. Further analysis revealed that a large number of genes associated with bacterial and fungal disease resistance responses were upregulated in the *cds1cds2* mutant lines. Further analysis revealed that a large number of genes associated with bacterial and fungal disease resistance responses were upregulated in the *cds1cds2* mutant lines. Many members of the *WRKY* transcription factor family, which serve as important signaling factors, were upregulated in the *cds1cds2* mutant (Figure 4d). The growth and immune regulator gene *BSK1* and the regulator gene *GLYI4*, which related to the JA and SA pathway were upregulated in *cds1cds2* (Figure 4b,d). The upregulation of these immune signal-related genes in the *cds1cds2* mutant regulated the immune response of the *cds1cds2* mutant and enhanced resistance to pathogens. Our data suggest that *AtS40*, *NGAL2*, *RGL3*, and other genes associated with embryonic development and growth in plants were also affected in the *cds1cds2* mutant (Figure 4b).
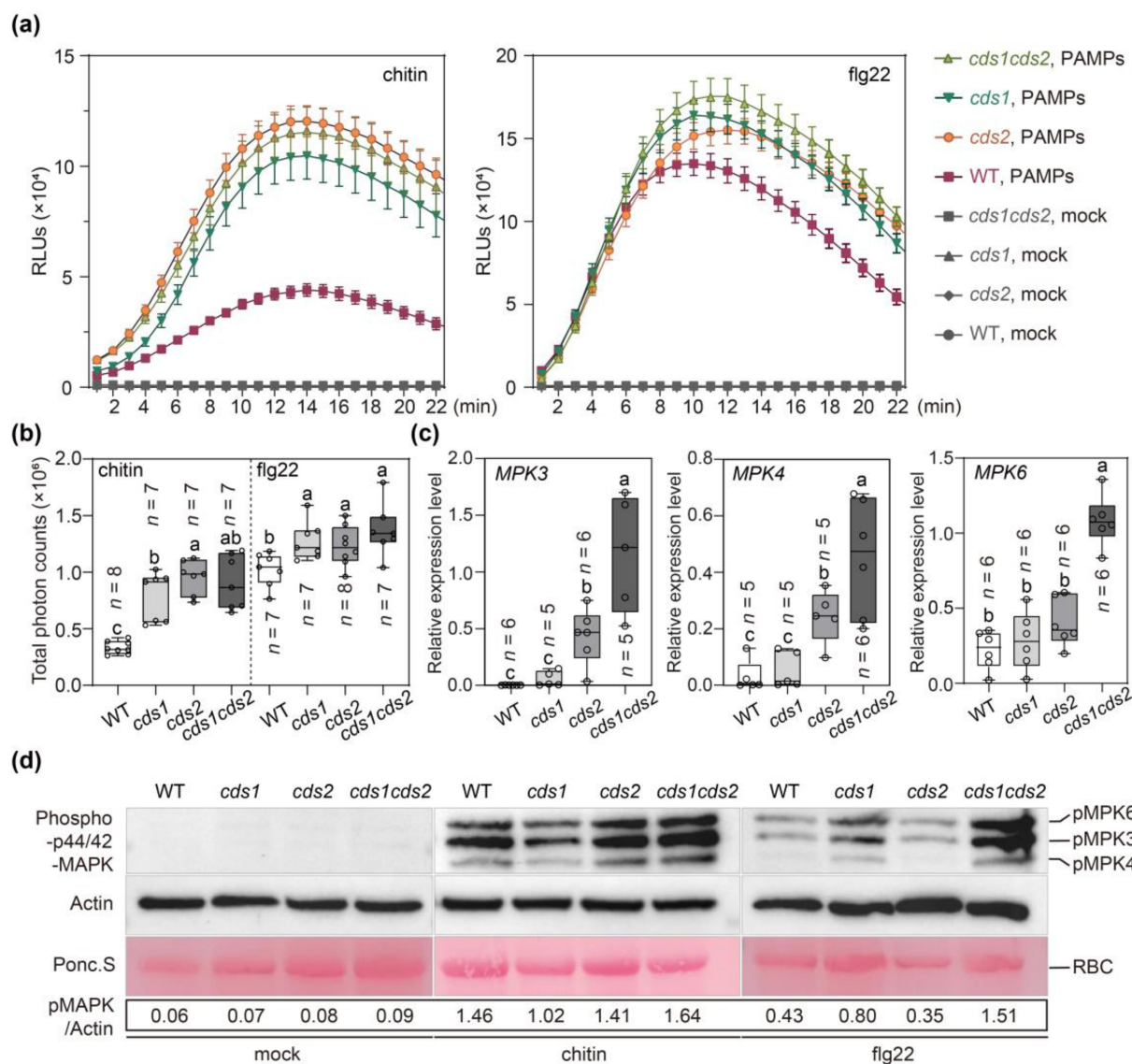
Figure 3. Plant immunity markers activated in *cds* mutants. (a) Reactive oxygen species (ROS) generation in *cds* mutant lines treated with chitin (120 nM) flg22 (200 nM) or water (mock); RLU, relative light unit. Leaves of 3-week-old *Arabidopsis* plants were used in the assays. Error bars represent mean ± SEM. (b) Total photon counts in *cds* mutant lines from (a). (c) RT-qPCR analyses of *MPK3*, *MPK4*, and *MPK6* expression levels in *cds* mutant lines. *ACTIN2* was used as the internal reference gene. (d) Immunoblot assays of MAPKs phosphorylation in *cds* leaves treated with chitin, flg22 and water (mock), respectively. RBC, ribulose-1,5-bis-phosphate carboxylase/oxygenase. Phosphorylated MAPKs were detected with the anti-phospho-p44/42 antibody, and goat anti-rabbit IgG HRP was used as the secondary antibody. Ponceau S staining shows the protein loading for each lane. Numbers below ponceau S stain indicate the band intensity relative to that of actin.

Metabolomics analyses were conducted to further investigate the effects of *CDS* genes mutation on plant metabolism. These analyses revealed many changes in key metabolites that are likely involved in immunity and growth (Figure 4c). The levels of serotonin, 5-Methoxyindole, and quercetin were elevated in the *cds1cds2* mutant (Figure 4c). These substances have been reported to play important roles in the immune and disease resistance responses of plants or to possess antibacterial, antioxidant, and antiviral activities. Some metabolites with antibacterial activity, such as 9-HPODE, O-Methylsinapic acid, and sinapinic acid, were elevated in the *cds1cds2* mutants as potential plant phytoalexins.[29–31] The *cds1cds2* mutant showed a significant accumulation of ABA, an important phytohormone that plays a key physiological role in regulating seed development, growth inhibition, promoting flower, and fruit drop.[32] Lipidomics results were consistent with previous reports that downregulation of *CDS1* and *CDS2* expression leads to PA accumulation and suppression of PI biosynthesis. As compared to WT, the relative content of PA was significantly higher, while the accumulation of PI was reduced in *cds1cds2* mutants. Both PA and PI have diverse roles, and altered levels of PA and PI might be a major cause of the alterations in the genes and metabolites mentioned above (Figure 4d). The decreased levels of diacylglycerol phospholipids (DAG) and Lysophosphatidylglycerol (LPG) were observed in *cds1cds2* mutant lines. The levels of Lysophosphatidylethanolamine (LPE), Lysophosphatidylcholine (LPC), Phosphatidylcholine (PC), as well as many other phospholipids, were increased in the *cds1cds2* mutant lines (Fig. S2). These transcriptomics and metabolomics results provide further evidence that *CDS*
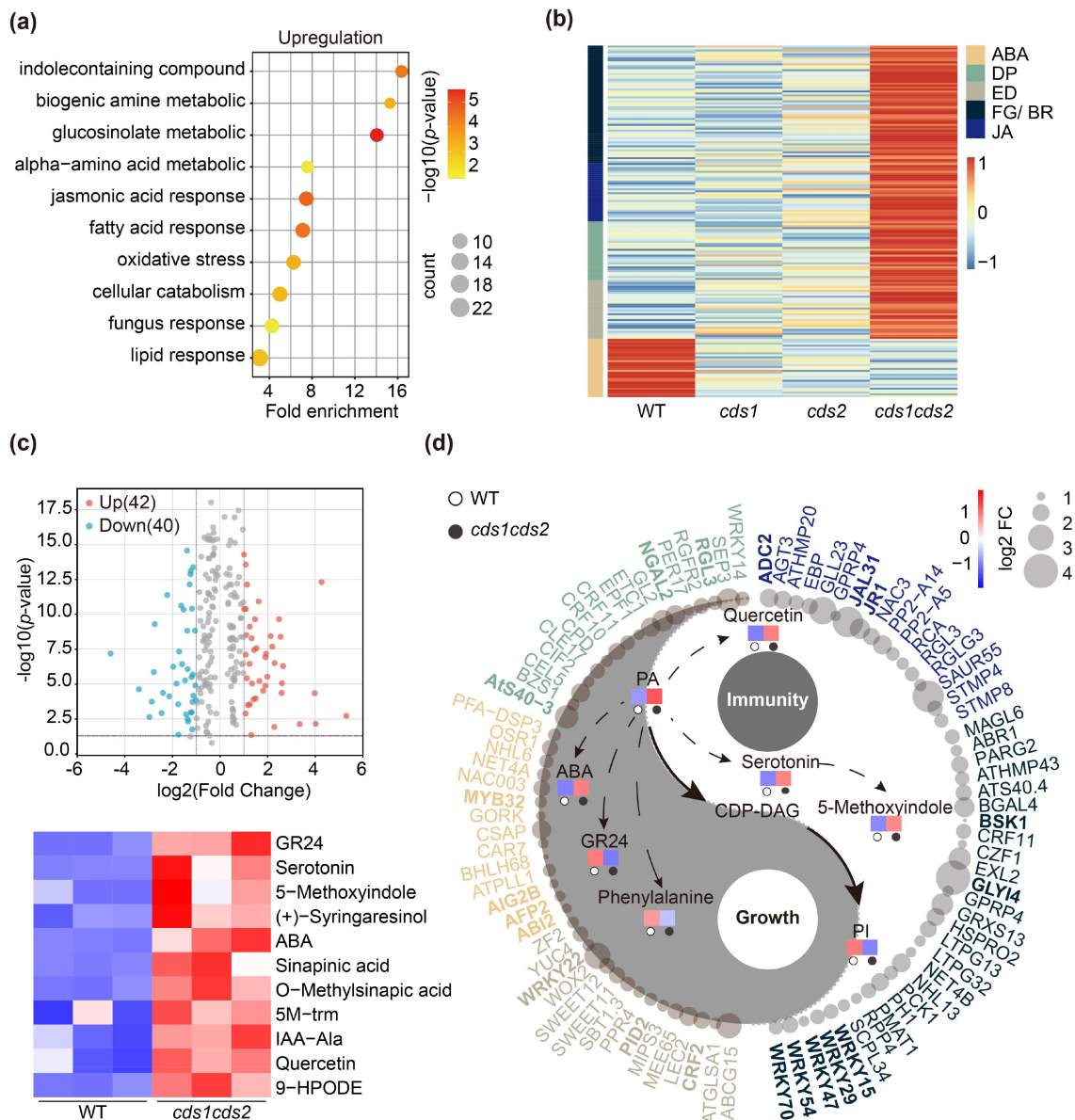
Figure 4. Integrated transcriptomics and metabolomics analyses of *cds1cds2*. (a) Gene ontology (GO) enrichment analysis of upregulated differentially expressed genes (DEGs) in *cds1cds2*. (b) Growth and immunity associated genes were upregulated in *cds1cds2*. ABA, abscisic acid response; DP, developmental process; ED, embryo development; FG/BR, fungus/bacterium defense response; JA, jasmonic acid response. (c) Volcano plots of differential metabolites in *cds1cds2 vs*. WT. (|Log2FC| ≥ 1.0, *p*-value ≤0.05). The heat map shows the relative levels of metabolites associated with growth and immunity in WT and *cds1cds2* mutant lines. Each lane in heatmap shows the replicate of WT and *cds1cds2* mutant. (d) Differential metabolites and DEGs associated with plant growth and immunity in *cds1cds2*. The colors in the box indicate the relative amounts of metabolites in the WT and *cds1cds2* lines. The size of the circle indicates the relative expression levels of the gene.

genes are negative regulators of immunity. Furthermore, the disruption of PA metabolic processes resulted in pleiotropic effects on growth and immunity, with a wide range of transcriptomics and metabolic changes.

4. Discussion

Previous studies have shown that loss of function of one of the *AtCDS1* and *AtCDS2* genes does not significantly affect *Arabidopsis* growth. Complete knockout of both *AtCDS1* and *AtCDS2* genes results in seedling lethality in *Arabidopsis*,[10] suggesting these genes are functionally redundant. Recently, *Arabidopsis* T-DNA insertional mutants with partial loss of *CDS1* and *CDS2* function were characterized, exhibiting defects

in embryonic development.[12] Here, we showed that the *cds1cds2* double mutant exhibited significantly impaired growth, manifesting in reduced plant height and diminished yield compared to the WT (Figure 1). These phenotypic changes may be attributed to defects in early embryonic development. Our results suggested that the *cds1cds2* mutant exhibited enhanced in broad-spectrum resistance (Figure 2) and displayed more robust immune response compared to the WT (Figure 3). These findings were consistent with previous results demonstrating that the *cds1cds2* mutant shows enhanced resistance to oomycetes. In rice, mutation of the CDP-DAG synthase gene *RBL1* results in lesion mimic phenotype and confers broad-spectrum disease resistance.[13] Similarly, mutations of the rice *OsCDS5* gene enhances ROS production and promotes expression levels of multiple defense-related genes, and

the *oscds5* mutant exhibits enhanced resistance to rice blast, bacterial blight, and bacterial leaf streak.[33] Through our studies in rice and *Arabidopsis*, we implied that partial loss of function of the *CDS* genes enhances plant resistance to diverse pathogens, underscoring the conserved roles of CDP-DAG synthase in regulating plant immunity.

The enhanced immunity of the *cds1cds2* mutant could be a result of metabolic changes in multiple pathways. Previous findings indicate that PA, a signaling molecule in plant immunity,[9] interacts with RBOH, subsequently activates downstream MPK3 and MPK6, promoting ROS production and MAPK phosphorylation to enhance disease resistance.[7] The level of PA was increased, as was the production of ROS and the levels of MAPK phosphorylation in the *cds1cds2* mutant, suggested the partial loss of CDS1 and CDS2 function in the *cds1cds2* mutant led to the accumulation of PA, which activated the downstream ROS and MAPK pathways that conferred disease resistance to the *cds1cds2* mutant. Alternatively, the enhanced immunity observed in the *cds1cds2* mutant may be attributed to the reduced PI levels. PI derivatives are modulated by plant pathogens to facilitate infection and are considered disease susceptibility factors. One of the PI derivates, PI(4,5)P$_2$, is recruited to the extrahaustorial membrane at powdery mildew infection sites to facilitate infection.[34] Mutation of PI(4,5)P$_2$ biosynthetic enzymes causes reduced PI(4,5)P$_2$ levels and enhanced resistance. In the *rbl1* rice mutant, reduced levels of PI and PIPs are observed, and the formation of cellular structures involved in pathogen effector protein translocation is disrupted, thereby resulting in enhanced immunity to multiple pathogens.[35] The level of PIPs requires to be measured, and the role of PIPs in enhanced immunity of the *cds1cds2* mutant requires further investigation. LPE, a natural occurring phospholipid, has been demonstrated to play a significant role in modulating early stages of plant senescence, primarily by delaying senescence-associated processes. LPE-treatment induces the signaling of SA and diverse immune defense responses, enhancing resistance to *Pst* DC3000 of *Arabidopsis*.[36] The increased levels of LPE and SA in the *cds1cds2* mutants suggested that the enhanced resistance in the *cds1cds2* mutants was achieved by accumulating LPE to activate the SA signaling pathway (Fig. S1-S2). Finally, the enhanced resistance observed in *Arabidopsis cds1cds2* mutant is potentially linked to the upregulation of immunity-related genes and the increased accumulation of defense-associated metabolites. Our integrated transcriptomics, lipidomics, and metabolomics analyses showed that the *WRKY* transcription factors, *BSK1*, and *GLYI4* were significantly upregulated in *cds1cds2* plants, which reportedly activated JA and SA signaling pathways and enhanced disease resistance in *Arabidopsis* (Figure 4b,d). *WRKY* transcription factors, the important signaling factors for MAPK-mediated disease resistance responses, which regulate plant immune responses through promoting the expression of *SARD1* and *CBP60* in *Arabidopsis*.[37] BSK1 plays a key role in growth and immune regulation by binding to BRI1 (the receptor of brassinosteroid, which regulates plant growth and development) and FLS2 (the receptor that perceives flagellin 22 to activate a series of downstream immune responses).[38] *GLYI4* is involved in the interaction between JA and SA pathways and enhances disease

resistance in *Arabidopsis*.[39] Our data indicated that the levels of some genes related to *Arabidopsis* growth have changed in the *cds1cds2* mutant. *RGL3*, a negative regulator of gibberellic acid signaling that inhibits plant growth and development, was upregulated in *cds1cds2*. *AtS40* and *NGAL2* were also upregulated in *cds1cds2*; *AtS40* plays a conducive role in plant senescence, and *NGAL2* inhibits seed development.[40–42] The significant accumulation of SA in *cds1cds2* mutants corroborated the activation of SA-mediated immune responses, underscoring the role of SA as a key signaling molecule (Fig. S1). Serotonin and 5-Methoxyindole were elevated in *cds1cds2*, which are plant defense-associated metabolites (Figure 4c,d). The accumulation of serotonin significantly enhances disease resistance in the rice *osspl5* mutant.[43] 5-Methoxyindole, a congener of melatonin, inhibits the growth, formation, and conidial germination of the fungal pathogen *Fusarium graminearum* and exhibits potent anti-fungal activity.[44] Quercetin, a plant hormone with suggests antimicrobial, antioxidant, and antiviral activities,[45] was increased in the *cds1cds2* mutant. Our findings suggest that the enhanced immunity observed in *Arabidopsis cds1cds2* mutant was attributable to multiple factors including elevated ROS production, increased MAPK phosphorylation, reduced PI levels, and upregulation of defense-related genes and metabolites.

Knock-down mutations of both *Arabidopsis CDS1* and *CDS2* genes enhanced plant immunity but reduced plant growth. In rice, the partially functional *CDS* gene confers broad-spectrum disease resistance without compromising yield.[13] Additionally, by editing the upstream open reading frame (uORF) of the gene, it may be possible to regulate protein abundance. For example, the introduction of uORF regulatory elements with inhibitory activities into the immunoregulatory factor of *Arabidopsis* modulates the protein translation level of AtNPR1, thereby improving broad-spectrum plant disease resistance without affecting growth and development.[46] Using such strategies, we anticipate that fine-tuning *CDS* transcript or protein abundance to balance growth and immunity in crops could then be applied to breeding programs for crops as novel sources of disease resistance.

Disclosure statement

No potential conflict of interest was reported by the author(s).

Author contributions

G.L. and G.S. designed the experiments. J.C. provided the *S. sclerotiorum* strain. R.T., X.L. and J.C. performed pathogen infection assays on *Arabidopsis*. G.S., Q.G. and R.T. performed MAPK phosphorylation assays. H.X. and X.D, generated transgenic plants. R. T. performed *Arabidopsis* growth phenotypic analyses, ROS and RT-qPCR assays. R.T., Q.G. and Q.L. performed lipid extraction and lipidomics analysis. G.S., W.Y., L.Y. and R.T. performed bioinformatics and RNA-seq data analyses. G.S., R.T., Y.L. and J.L. performed metabolomics profiling analyses and SA analyses. G.L., G.S. and R.T. drafted the manuscript. G.L., G.S., Q.G. and R.T. revised the manuscript with inputs from all authors. All authors read and approved the final manuscript.

Data availability statement

The genes mentioned in this study are as follows: *AtCDS1* (AT1G62430, CP138171.1); *AtCDS2* (AT4G22340, CP138174.1). RNA-seq data are available in the National Center for Biotechnology Information (NCBI) (http://www.ncbi.nlm.nih.gov/) under the accession number of PRJNA1091892.

ORCID

Ronglei Tan http://orcid.org/0009-0009-1543-8455
Gan Sha http://orcid.org/0009-0008-1966-8656
Guotian Li http://orcid.org/0000-0001-6780-7085

References

1. Xing J, Zhang L, Duan Z, Lin J. Coordination of phospholipid-based signaling and membrane trafficking in plant immunity. Trends Plant Sci. 2021;26(4):407–420. doi:10.1016/j.tplants.2020.11.010.

2. Ali U, Lu S, Fadlalla T, Iqbal S, Yue H, Yang B, Hong Y, Wang X, Guo L. The functions of phospholipases and their hydrolysis products in plant growth, development and stress responses. Prog Lipid Res. 2022;86:101158. doi:10.1016/j.plipres.2022.101158.

3. Yao S, Kim SC, Li J, Tang S, Wang X. Phosphatidic acid signaling and function in nuclei. Prog Lipid Res. 2024;93:101267. doi:10.1016/j.plipres.2023.101267.

4. Qi F, Li J, Ai Y, Shangguan K, Li P, Lin F, Liang Y. DGK5β-derived phosphatidic acid regulates ROS production in plant immunity by stabilizing NADPH oxidase. Cell Host Microbe. 2024;32(3):425–440.e7. doi:10.1016/j.chom.2024.01.011.

5. Zhang Y, Zhu H, Zhang Q, Li M, Yan M, Wang R, Wang L, Welti R, Zhang W, Wang X. Phospholipase Dα1 and phosphatidic acid regulate NADPH oxidase activity and production of reactive oxygen species in aba-mediated stomatal closure in Arabidopsis. The Plant Cell. 2009;21(8):2357–2377. doi:10.1105/tpc.108.062992.

6. Li J, Wang X. Phospholipase D and phosphatidic acid in plant immunity. Plant Sci. 2019;279:45–50. doi:10.1016/j.plantsci.2018.05.021.

7. Kong L, Ma X, Zhang C, Kim SI, Li B, Xie Y, Yeo I-C, Thapa H, Chen S, Devarenne TP, et al. Dual phosphorylation of DGK5-mediated PA burst regulates ROS in plant immunity. Cell. 2024;187(3):609–623.e21. doi:10.1016/j.cell.2023.12.030.

8. Li J, Yao S, Kim SC, Wang X. Lipid phosphorylation by a diacylglycerol kinase suppresses ABA biosynthesis to regulate plant stress responses. Mol Plant. 2024;17(2):342–358. doi:10.1016/j.molp.2024.01.003.

9. Jennings W, Epand RM. Cdp-diacylglycerol, a critical intermediate in lipid metabolism. Chem Phys Lipids. 2020;230:104914. doi:10.1016/j.chemphyslip.2020.104914.

10. Zhou Y, Peisker H, Weth A, Baumgartner W, Dörmann P, Frentzen M. Extraplastidial cytidinediphosphate diacylglycerol synthase activity is required for vegetative development in Arabidopsis thaliana. Plant J. 2013;75(5):867–879. doi:10.1111/tpj.12248.

11. Haselier A, Akbari H, Weth A, Baumgartner W, Frentzen M. Two closely related genes of Arabidopsis encode plastidial cytidinediphosphate diacylglycerol synthases essential for photoautotrophic growth. Plant Physiol. 2010;153(3):1372–1384. doi:10.1104/pp.110.156422.

12. Du XQ, Yao HY, Luo P, Tang XC, Xue HW, Qu L-J. Cytidinediphosphate diacylglycerol synthase—mediated phosphatidic acid metabolism is crucial for early embryonic development of Arabidopsis. PloS Genet. 2022;18(7):e1010320. doi:10.1371/journal.pgen.1010320.

13. Sha G, Sun P, Kong X, Han X, Sun Q, Fouillen L, Zhao J, Li Y, Yang L, Wang Y, et al. Genome editing of a rice CDP-DAG synthase confers multipathogen resistance. Nature. 2023;618 (7967):1017–1023. doi:10.1038/s41586-023-06205-2.

14. Kamaruzzaman M, He G, Wu M, Zhang J, Yang L, Chen W, Li G. A novel partitivirus in the hypovirulent isolate QT5-19 of the plant pathogenic fungus botrytis cinerea. Viruses. 2019;11(1):11. doi:10.3390/v11010024.

15. Gong Y, Fu Y, Xie J, Li B, Chen T, Lin Y, Chen W, Jiang D, Cheng J. Sclerotinia sclerotiorum SsCut1 modulates virulence and cutinase activity. J Fungi. 2022;8(5):526. doi:10.3390/jof8050526.

16. Yuan M, Jiang Z, Bi G, Nomura K, Liu M, Wang Y, Cai B, Zhou J-M, He SY, Xin X-F. Pattern-recognition receptors are required for nlr-mediated plant immunity. Nature. 2021;592 (7852):105–109. doi:10.1038/s41586-021-03316-6.

17. Hu Y, Ding Y, Cai B, Qin X, Wu J, Yuan M, Wan S, Zhao Y, Xin X-F. Bacterial effectors manipulate plant abscisic acid signaling for creation of an aqueous apoplast. Cell Host & Microbe. 2022;30 (4):518–529.e6. doi:10.1016/j.chom.2022.02.002.

18. Liu Q, Ning Y, Zhang Y, Yu N, Zhao C, Zhan X, Wu W, Chen D, Wei X, Wang G-L, et al. OsCUL3a negatively regulates cell death and immunity by degrading OsNPR1 in rice. Plant Cell. 2017;29 (2):345–359. doi:10.1105/tpc.16.00650.

19. Livak KJ, Schmittgen TD. Analysis of relative gene expression data using real-time quantitative PCR and the $2-\Delta\Delta CT$ method. Methods. 2001;25(4):402–408. doi:10.1006/meth.2001.1262.

20. Zhai K, Liang D, Li H, Jiao F, Yan B, Liu J, Lei Z, Huang L, Gong X, Wang X, et al. NLRs guard metabolism to coordinate pattern- and effector-triggered immunity. Nature. 2022;601(7892):245–251. doi:10.1038/s41586-021-04219-2.

21. Huang J, Liang X, Xuan Y, Geng C, Li Y, Lu H, Qu S, Mei X, Chen H, Yu T, et al. A reference human genome dataset of the BGISEQ-500 sequencer. Gigascience. 2017;6(5):1–9. doi:10.1093/gigascience/gix024.

22. Yu G, Wang LG, Han Y, He QY. clusterProfiler: an R package for comparing biological themes among gene clusters. Omics A J Intgr Biol. 2012;16(5):284–287. doi:10.1089/omi.2011.0118.

23. Hong Y, Yuan S, Sun L, Wang X, Hong Y. Cytidinediphosphate-diacylglycerol synthase 5 is required for phospholipid homeostasis and is negatively involved in hyperosmotic stress tolerance. Plant J. 2018;94(6):1038–1050. doi:10.1111/tpj.13916.

24. Zhao J, Chen Y, Ding Z, Zhou Y, Bi R, Qin Z, Yang L, Sun P, Sun Q, Chen G, et al. Identification of propranolol and derivatives that are chemical inhibitors of phosphatidate phosphatase as potential broad-spectrum fungicides. Plant Commun. 2024;5(1):100679. doi:10.1016/j.xplc.2023.100679.

25. Lu S, Liu H, Jin C, Li Q, Guo L. An efficient and comprehensive plant glycerolipids analysis approach based on high-performance liquid chromatography–quadrupole time-of-flight mass spectrometer. Plant Direct. 2019;3(11):e00183. doi:10.1002/pld3.183.

26. Zhang F, Guo H, Huang J, Yang C, Li Y, Wang X, Qu L, Liu X, Luo J. A UV-B-responsive glycosyltransferase, OsUGT706C2, modulates flavonoid metabolism in rice. Sci China Life Sci. 2020;63(7):1037–1052. doi:10.1007/s11427-019-1604-3.

27. Zhou J, Liu C, Chen Q, Liu L, Niu S, Chen R, Li K, Sun Y, Shi Y, Yang C, et al. Integration of rhythmic metabolome and transcriptome provides insights into the transmission of rhythmic fluctuations and temporal diversity of metabolism in rice. Sci China Life Sci. 2022;65(9):1794–1810. doi:10.1007/s11427-021-2064-7.

28. Li Y, Yang Z, Yang C, Liu Z, Shen S, Zhan C, Lyu Y, Zhang F, Li K, Shi Y, et al. The NET locus determines the food taste, cooking and nutrition quality of rice. Sci Bull. 2022;67(20):2045–2049. doi:10.1016/j.scib.2022.09.023.

29. Chen C. Sinapic acid and its derivatives as medicine in oxidative stress-induced diseases and aging. Oxid Med Cell Longev. 2016, 2016;2016(1):3571614. doi:10.1155/2016/3571614.

30. Kimura H, Yokota K. Characterization of metabolic pathway of linoleic acid 9-hydroperoxide in cytosolic fraction of potato tubers and identification of reaction products. Appl Biochem Biotechnol. 2004;118(1–3):115–132. doi:10.1385/ABAB:118:1-3:115.

31. Zhao Z, Song H, Xie J, Liu T, Zhao X, Chen X, He X, Wu S, Zhang Y, Zheng X. Research progress in the biological activities of 3,4,5-trimethoxycinnamic acid (TMCA) derivatives. Eur J Med Chem. 2019;173:213–227. doi:10.1016/j.ejmech.2019.04.009.

32. Luo X, Chen Z, Gao J, Gong Z. Abscisic acid inhibits root growth in Arabidopsis through ethylene biosynthesis. Plant J. 2014;79(1):44–55. doi:10.1111/tpj.12534.

33. Sun Q, Xiao Y, Song L, Yang L, Wang Y, Yang W, Yang Q, Xie K, Yuan M, Li G. Mutation of OsCDS5 confers broad-spectrum disease resistance in rice. Mol Plant Pathol. 2024;25(2):e13430. doi:10.1111/mpp.13430.

34. Qin L, Zhou Z, Li Q, Zhai C, Liu L, Quilichini TD, Gao P, Kessler SA, Jaillais Y, Datla R, et al. Specific recruitment of phosphoinositide species to the plant-pathogen interfacial membrane underlies Arabidopsis susceptibility to fungal infection. Plant Cell. 2020;32(5):1665–1688. doi:10.1105/tpc.19.00970.

35. Sha G, Li G. Effector translocation and rational design of disease resistance. Trends Microbiol. 2023;31(12):1202–1205. doi:10.1016/j.tim.2023.09.007.

36. Völz R, Park JY, Harris W, Hwang S, Lee YH. Lyso-phosphatidylethanolamine primes the plant immune system and promotes basal resistance against hemibiotrophic pathogens. BMC Biotechnol. 2021;21(1):12. doi:10.1186/s12896-020-00661-8.

37. Chen S, Ding Y, Tian H, Wang S, Zhang Y. WRKY54 and WRKY70 positively regulate SARD1 and CBP60g expression in plant immunity. Plant Signal Behav. 2021;16(10):1932142. doi:10.1080/15592324.2021.1932142.

38. Su B, Zhang X, Li L, Abbas S, Yu M, Cui Y, Baluška F, Hwang I, Shan X, Lin J. Dynamic spatial reorganization of BSK1 complexes in the plasma membrane underpins signal-specific activation for growth and immunity. Mol Plant. 2021;14(4):588–603. doi:10.1016/j.molp.2021.01.019.

39. Proietti S, Falconieri GS, Bertini L, Baccelli I, Paccosi E, Belardo A, Timperio AM, Caruso C. GLYI4 plays a role in methylglyoxal detoxification and jasmonate-mediated stress responses in Arabidopsis thaliana. Biomolecules. 2019;9(10):635. doi:10.3390/biom9100635.

40. Fischer-Kilbienski I, Miao Y, Roitsch T, Zschiesche W, Humbeck K, Krupinska K. Nuclear targeted AtS40 modulates senescence associated gene expression in Arabidopsis thaliana during natural development and in darkness. Plant Mol Biol. 2010;73(4–5):379–390. doi:10.1007/s11103-010-9618-3.

41. Wild M, Achard P. The DELLA protein RGL3 positively contributes to jasmonate/ethylene defense responses. Plant Signal Behav. 2013;8(4):e23891. doi:10.4161/psb.23891.

42. Zhang Y, Du L, Xu R, Cui R, Hao J, Sun C, Li Y. Transcription factors SOD7/NGAL2 and DPA4/NGAL3 act redundantly to regulate seed size by directly repressing KLU expression in Arabidopsis thaliana. Plant Cell. 2015;27(3):620–632. doi:10.1105/tpc.114.135368.

43. Jin B, Zhou X, Jiang B, Gu Z, Zhang P, Qian Q, Chen X, Ma B. Transcriptome profiling of the spl5 mutant reveals that SPL5 has a negative role in the biosynthesis of serotonin for rice disease resistance. Rice. 2015;8(1):18. doi:10.1186/s12284-015-0052-7.

44. Kong M, Liang J, Ali Q, Wen W, Wu H, Gao X, Gu Q. 5-methoxyindole, a chemical homolog of melatonin, adversely affects the phytopathogenic fungus Fusarium graminearum. Int J Mol Sci. 2021;22(20):10991. doi:10.3390/ijms222010991.

45. Singh P, Arif Y, Bajguz A, Hayat S. The role of quercetin in plants. Plant Physiol Biochem. 2021;166:10–19. doi:10.1016/j.plaphy.2021.05.023.

46. Zhang H, Si X, Ji X, Fan R, Liu J, Chen K, Wang D, Gao C. Genome editing of upstream open reading frames enables translational control in plants. Nat Biotechnol. 2018;36(9):894–898. doi:10.1038/nbt.4202.